applied sciences

MDPI

Article

Face Stability Analysis for Tunnels under Steady Unsaturated Seepage and Inhomogeneity Conditions

Yi Xie, Hong Liao and De Zhou *

School of Civil Engineering, Central South University, Changsha 410075, China; 234811064@csu.edu.cn (Y.X.); hnhsjc@163.com (H.L.)
* Correspondence: 210026@csu.edu.cn

Abstract: In the field of tunnels, the stability of tunnel faces is generally considered in dry, saturated and homogeneous soils. However, the actual condition of some soils has been found to be inhomogeneous, with unsaturated seepage. In this paper, an analytical method is applied to estimate the safety factor when the supporting force at the tunnel face is zero under steady unsaturated seepage and inhomogeneous conditions. This method combines kinematic limit analysis techniques with strength reduction techniques; an efficient stress formulation utilizing suction stress is employed to determine the apparent cohesive force to obtain the solution of the steady unsaturated seepage problem, and indicators of soil inhomogeneity are attributed to the effect on cohesion. A 3D log-spiral collapse mechanism is used to find the zero supporting pressure and determine the safety factor through an iterative method. This paper analyzes the effect of variations in the unsaturated parameters, inhomogeneity parameters and tunnel dimensional parameters on the stability of the tunnel face.

Keywords: tunnel; face stability; steady unsaturated seepage; inhomogeneous soil; safety factor

Citation: Xie, Y.; Liao, H.; Zhou, D. Face Stability Analysis for Tunnels under Steady Unsaturated Seepage and Inhomogeneity Conditions. *Appl. Sci.* **2024**, *14*, 9377. https://doi.org/10.3390/app14209377

Academic Editor: Tiago Miranda

Received: 1 September 2024
Revised: 19 September 2024
Accepted: 11 October 2024
Published: 14 October 2024

1. Introduction

The stability of the tunnel face is a crucial concern during the tunnel excavation process, which involves geotechnical engineering, underground engineering and other fields. In the process of tunnel excavation, firstly, different engineering designs and construction techniques, and secondly, complex geological conditions, such as the fracture and slip of surrounding rock, the inhomogeneity of soils, seepage and other factors, are considered to have an impact on the stability of the tunnel face.

Many researchers have put forward a variety of failure mechanisms for stability problems of the tunnel face. A failure model for rigid conical blocks under the limit analysis theorem have supplied a solution that encompasses a considerable number of blocks. More precise solutions were achieved by Mollon et al. (2010) [1] through the integration of additional blocks. A "horn-like" failure model for assessing tunnel face stability was proposed by Subrin and Wong (2002) [2]. Spatial discretization was used by Mollon et al. (2011) [3] to develop a 3D discrete model that is more representative of engineering reality; however, this solution is overly complex and time-consuming. A triangular-based prism model for the safety evaluation of shallow tunnel faces was raised by Oreste and Dias (2012) [4]. Classical silo and wedge mechanisms were utilized by Perazzelli et al. (2014) [5] to determine the necessary pressures on tunnel faces in saturated soils under seepage conditions. Yang and Yin (2004) [6] applied the upper bound theorem of plasticity to determine a rigorous upper limit for the stability factor under plane strain assumptions, utilizing a nonlinear yield criterion in calculations. Within the scope of the upper bound theorem (Yang and Huang, 2011) [7], Yang and Yin (2005) [8] utilized a nonlinear Hoek–Brown failure criterion, coupled with an innovative bending damage mechanism, to establish the collapse profile for shallow circular tunnels. Yang and Wang (2011) [9] harnessed the random medium theory to forecast the ground surface displacements resulting from tunneling activities, thereby assessing the stability of the

tunnel face. A new discretization technique was proposed by Xu et al. (2023) [10] for a three-dimensional (3D) tunnel face in weak strata with a random position in space. Many subsequent studies have been inspired by these fundamental failure mechanisms.

Numerous researchers have explored kinematic limit analysis methods, with Yang et al. (2004) [11] employing such an approach to assess the seismic and static stability of slopes. Integrating the suggested coefficients into the kinematic framework of limit analysis, Zhang and Wu (2023) [12] crafted a three-dimensional (3D) failure mechanism capable of capturing the full spectrum of potential instability scenarios.

Depending on the construction process, tunnels can be generally classified into two main types: closed-face and open-face. The primary distinction between the two types of tunnels is that face pressure generally exists for support on the face of closed-face tunnels, such as shield tunnels, which are often assessed with the necessary face pressures, while open-face tunnels do not need to be supported by face pressures, such as tunnels excavated with the New Austrian Tunneling Method, which are more appropriately assessed using a safety factor. This paper focuses exclusively on open-face tunnels to examine the safety factor under conditions of unsaturated seepage and soil inhomogeneity. In existing studies, two methods of safety factor calculation are proposed. The gravity increase method was used by Li et al. (2009) [13], with the safety factor defined as the ratio of the internal dissipated work rate to the external work rate. The strength reduction technique has been employed by many studies, defining the safety factor as the ratio of the initial soil strength to the soil strength at the ultimate collapse state. It has been shown that more conservative results can be produced by the strength reduction technique. Therefore, the strength reduction technique was employed in this paper.

Steady unsaturated soils were modeled by defining a friction angle φ^b, but it was experimentally demonstrated that φ^b varies with matric suction; however, assumptions about the matric suction distribution are inaccurate. A framework for the stress behavior of unsaturated soils based on a one-dimensional model of seepage and suction stress was established by Lu et al. (2010) [14] and Vahedifard et al. (2015) [15]. However, the above studies were mostly used for the assessment of slope stability and calculation of soil pressure, and did not address the issue of tunnel face stability.

Inhomogeneity refers to the variation in soil strength parameters with the change of three-dimensional coordinates, and this property is proved to be particularly obvious in the vertical direction. In this study, cohesion is assumed to vary vertically while remaining constant horizontally.

The impacts of steady unsaturated seepage and soil inhomogeneity are integrated into the stability analysis of the tunnel face in this study. To achieve this, the theory of generalized effective stress is employed to obtain the distribution of suction stress, while an extended Mohr–Coulomb failure criterion is utilized to determine the strength of unsaturated soils. In addition, an inhomogeneous cohesion model utilized by Nian et al. (2008) [16] is employed to simulate the inhomogeneous condition of the soil. For the sake of characterizing the stability condition of the tunnel face, a 3D log-spiral failure mechanism is applied. An iterative method was used to determine the safety factor within the framework of strength reduction techniques to find zero supporting pressure on the tunnel face. The effects of different parameter variations are discussed. The findings can serve as a foundation for future tunnel excavation design.

2. Derivation of Total Cohesion

A consolidated expression for effective stress was proposed by Lu and Likos (2004) [17] as follows:

$$\sigma' = \sigma - u_a - \sigma^s \quad (1)$$

where σ' is the effective stress, σ is the total stress, u_a is the pore air pressure and σ^s is the suction stress. Following standard practice, positive values are assigned to normal compressive stress.

Lu et al. (2010) [14] presented the expression for σ^s as follows:

$$\sigma^s = -(u_a - u_w) \tag{2a}$$

$$\sigma^s = -\frac{(u_a - u_w)}{\left\{1 + [\alpha(u_a - u_w)]^n\right\}^{(n-1)/n}} \tag{2b}$$

where u_w is the pore water pressure and the values of α and n are determined by the different types of soil, where α is the reciprocal of soil entry pressure, taking values between 0.001 kPa^{-1} and 0.5 kPa^{-1} and n is a parameter reflecting the distribution of soil pores; Vahedifard et al. (2015) [15] pointed out that n values should be in the range of 1.1–8.5. It is worth mentioning that Equation (2a) applies to the case when $(u_a - u_w) \leq 0$ and Equation (2b) applies to the case when $(u_a - u_w) > 0$; this means that Equation (2a) applies to soils that are fully saturated while Equation (2b) applies to soils that are unsaturated, so Equation (2b) was used for the following derivation.

Expressions describing the substrate suction were derived by Vahedifard et al. (2015) [15] and Griffiths and Lu (2005) [18] based on Darcy's law, in combination with the case for $z = 0$ when $(u_a - u_w) = 0$, which takes the following form:

$$(u_a - u_w) = -\frac{1}{\alpha}\ln\left[\left(1 + \frac{q}{k_s}\right)e^{-\gamma_w \alpha z} - \frac{q}{k_s}\right] \tag{3}$$

where q is the rate of steady unsaturated seepage, with infiltration for $q < 0$ and evaporation for $q > 0$, and k_s is saturated hydraulic conductivity. The simultaneous equation for Equations (2b) and (3) is as follows:

$$\sigma^s = \frac{1}{\alpha}\frac{\ln\left[\left(1 + \frac{q}{k_s}\right)e^{-\gamma_w \alpha z} - \frac{q}{k_s}\right]}{\left(1 + \left\{-\ln\left[\left(1 + \frac{q}{k_s}\right)e^{-\gamma_w \alpha z} - \frac{q}{k_s}\right]\right\}^n\right)^{(n-1)/n}} \tag{4}$$

On the basis of an extended form derived from the Mohr–Coulomb criterion (Vahedifard et al., 2015) [15], which describes the strength and the variation of unsaturated soils, the parameter called apparent cohesion was applied so as to obtain the shear strength component due to unsaturated seepage effects. The cohesion of unsaturated soils consists of an apparent cohesion (c_{app}) and an effective cohesion (c'), expressed as follows:

$$c_{app} = -\sigma^s \tan\varphi' \tag{5}$$

$$c = c' + c_{app} \tag{6}$$

For the case of inhomogeneous soils, an inhomogeneous cohesion model proposed by Nian et al. (2008) [16] and Pan and Dias (2016) [19] was employed, and so as to be consistent with the expression of the apparent cohesion, the model is rewritten as a function of z, which takes the following form:

$$c(z) = \begin{cases} n_0 c + \frac{c - n_0 c}{H}(C + D + z_0 - z) & (C + D + z_0 - H) < z \leq (C + D + z_0) \\ n_2 c - \frac{n_2 c - n_1 c}{C + D - H}(z - z_0) & z_0 \leq z \leq (C + D + z_0 - H) \end{cases} \tag{7}$$

where C is the vertical distance between the top of the tunnel and the ground, i.e., buried depth, D is the diameter of the tunnel, z_0 is the distance from the bottom of the tunnel excavation to the horizontal, z denotes the length measured vertically from the horizontal plane to the corresponding point on the failure mechanism's surface, c is the cohesion at a depth of H and n_0, n_1 and n_2 are coefficients reflecting the inhomogeneous character of the soil as follows:$n_0 = n_1 = n_2$ for soil with homogeneous cohesion, $n_1 = 1$, $n_2 = n_0 + (1 - n_0)(C + D)/H$ for soil whose cohesion varies linearly with vertical depth

and $n_1 \neq 1$ for soil with two layers. The second scenario is taken as the object of this study. Simplifying Equation (7) according to $n_1 = 1, n_2 = n_0 + (1 - n_0)(C + D)/H$ gives:

$$c(z) = c\left[n_0 + \frac{(1 - n_0)(C + D + z_0 - z)}{H}\right] \quad z_0 \leq z \leq (C + D + z_0) \tag{8}$$

Combining Equations (4), (5), (6) and (8) yields an expression for total cohesion under steady unsaturated seepage and inhomogeneity conditions as follows:

$$c_{total} = c'\left[n_0 + \frac{(1 - n_0)(C + D + z_0 - z)}{H}\right] - \tan\varphi' \frac{1}{\alpha} \frac{\ln\left[\left(1 + \frac{q}{k_s}\right)e^{-\gamma_w \alpha z} - \frac{q}{k_s}\right]}{\left(1 + \left\{-\ln\left[\left(1 + \frac{q}{k_s}\right)e^{-\gamma_w \alpha z} - \frac{q}{k_s}\right]\right\}^n\right)^{(n-1)/n}} \tag{9}$$

3. 3D Logarithmic Spiral Failure Mechanism

The scenario examined in this paper is illustrated in Figure 1. It involves a tunnel with a lack of face support pressure, characterized by a diameter of D and a cover depth of C. The soil surrounding the tunnel exhibits steady unsaturated seepage and inhomogeneity conditions. The horizontal plane is located at a vertical distance z_0 from the bottom of the tunnel.

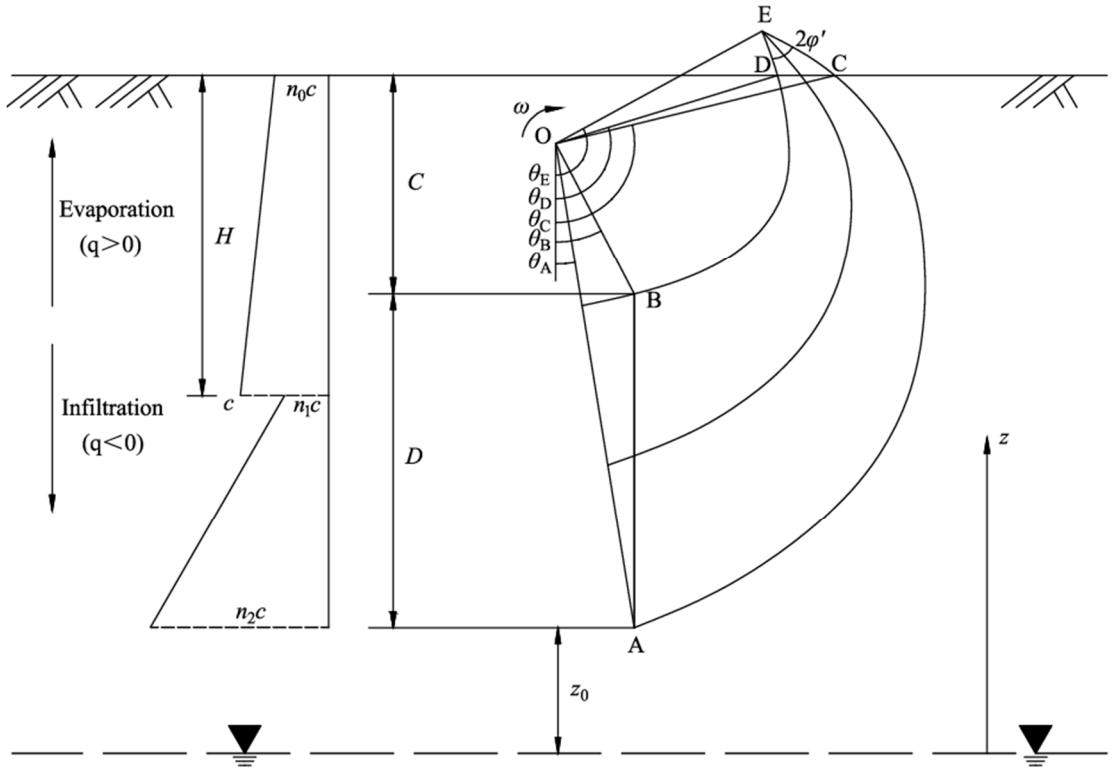

Figure 1. Diagram of the analyzed situation in the longitudinal section of the failure mechanism.

The kinematic limit analysis method is employed in this research, with the primary focus on establishing an effective collapse mechanism. It is assumed that the soil obeys the rule of associative flow, which indicates that the velocity vector should be positioned at an angle corresponding to the effective internal friction angle of the sliding surface, hence v_n can be expressed as:

$$v_n = v_t \tan\varphi' \tag{10}$$

where v_n represents the normal component of the velocity on the sliding surface, while v_t denotes the tangential component. Equation (10) indicates that during rigid rotation, the mechanism's profile forms a logarithmic spiral curve, and the sliding surface is a

tangent to a cone with a summit angle of $2\varphi'$. Consequently, the mechanism is employed to characterize the failure of the face.

The mechanism rotates with angular velocity ω around the centre of rotation O. Therefore, it is necessary to set up a polar coordinate system (θ, ρ) and represent the velocity at any point within the mechanism as:

$$v = \omega\rho \tag{11}$$

The traces of this mechanism are controlled by two logarithmic spiral curves: curves AE and BE. These can be expressed as follows:

curves AE:

$$r = r_A e^{-(\theta-\theta_A)\tan\varphi'} \tag{12}$$

curves BE:

$$r' = r_B e^{(\theta-\theta_B)\tan\varphi'} \tag{13}$$

where r_A and r_B can be represented by θ_A and θ_B, as follows:

$$\begin{cases} r_A = \frac{\sin\theta_B}{\sin(\theta_B-\theta_A)}D \\ r_B = \frac{\sin\theta_A}{\sin(\theta_B-\theta_A)}D \end{cases} \tag{14}$$

The logarithmic spiral mechanism is formed by a number of circles, which are centered on the points on the rotation axis of the two logarithmic spiral curves; the traces of the center points can be represented as:

$$r_m = \frac{r + r\prime}{2} \tag{15}$$

and the radius of the circle can be determined as follows:

$$R = \frac{r - r\prime}{2} \tag{16}$$

Two logarithmic spiral curves intersect at point E, which can be represented by the following polar coordinates:

$$\begin{cases} \theta_E = \frac{\theta_A+\theta_B}{2} + \frac{\ln(\sin\theta_B/\sin\theta_A)}{2\tan\varphi'} \\ r_E = \frac{\sqrt{\sin\theta_A\sin\theta_B}}{\sin(\theta_B-\theta_A)} e^{\frac{1}{2}(\theta_A-\theta_B)\tan\varphi'} D \end{cases} \tag{17}$$

In some tunnels with shallow depths, the failure mechanism may outcrop, in which case the intersections of curves AE and BE with the ground are C and D, respectively. In this case, the mechanism is controlled by the curves AC and BD as well as the ground CD. The positions of points C and D on the ground can be represented by θ_C and θ_D as follows:

$$\begin{cases} r_B\cos\theta_B - r_A\cos\theta_C e^{-(\theta_C-\theta_A)\tan\varphi'} = C \\ r_B\cos\theta_B - r_B\cos\theta_D e^{(\theta_D-\theta_B)\tan\varphi'} = C \end{cases} \tag{18}$$

Accordingly, θ_A and θ_B are chosen as optimization variables describing the failure mechanism, and they need to satisfy the following conditions:

$$\begin{cases} 0 < \theta_A < \theta_B < \frac{\pi}{2} \\ \theta_B < \theta_E < \pi \end{cases} \tag{19}$$

4. Strength Reduction Technique

The safety factor was defined as the ratio of the original soil strength to the reduced soil strength when the tunnel face reaches the ultimate critical condition of collapse. The safety factor is expressed according to this definition as:

$$FS = \frac{\tan\varphi'}{\tan\varphi'_d} = \frac{c'}{c'_d} \tag{20}$$

where FS is the safety factor and φ'_d and c'_d are the parameters of the strength reduction for the ultimate critical state of collapse. In the parameter process, the soil strength is increased or decreased as a result of the variation in the value of FS until the pressure on the tunnel face reaches zero, i.e., $\sigma_c = 0$. The general formula for σ_c can be determined as:

$$\sigma_c = \max\left\{ \frac{\dot{W}_\gamma - \dot{D}}{2\omega r_A^2 \sin^2\theta_A \int_{\theta_A}^{\theta_B} \sqrt{R^2 - d_1^2}\cot\theta\csc^2\theta d\theta} \right\} \tag{21}$$

Here, $\dot{W}_\gamma$ represents the external work rate performed by the collapsing soil gravity, while $\dot{D}$ denotes the internal dissipation rate resulting from the total cohesion, i.e., c_{total} in Equation (9). It is worth noting that c_{total} is a function of z, which represents the perpendicular distance from a point on the failure mechanism to the horizontal plane. z can be expressed as:

$$z = r_A\cos\theta_A - (r_m + y)\cos\theta + z_0 \tag{22}$$

The rate of internal work is derived as:

$$\begin{aligned}\dot{D} = 2\omega \Bigg[&\int_{\theta_A}^{\theta_B}\int_{d_1}^{R} c_{total}\frac{R(r_m+y)^2}{\sqrt{R^2-y^2}}dyd\theta + \int_{\theta_B}^{\theta_C}\int_{-R}^{R} c_{total}\frac{R(r_m+y)^2}{\sqrt{R^2-y^2}}dyd\theta \\ &+ \int_{\theta_C}^{\theta_D}\int_{-R}^{d_2} c_{total}\frac{R(r_m+y)^2}{\sqrt{R^2-y^2}}dyd\theta \Bigg]\end{aligned} \tag{23}$$

where d_1 and d_2 are the distances from the center O to points located on the face of the tunnel and on the surface of the ground, respectively, as expressed by the following equation:

$$\begin{cases} d_1 = r_A\frac{\sin\theta_A}{\sin\theta} - r_m \\ d_2 = r_C\frac{\sin\theta_C}{\sin\theta} - r_m \end{cases} \tag{24}$$

The rate of external work is derived as:

$$\begin{aligned}\dot{W}_\gamma = 2\omega\gamma \Bigg[&\int_{\theta_A}^{\theta_B}\int_{d_1}^{R}\int_0^{\sqrt{R^2-y^2}} (r_m+y)^2\sin\theta dxdyd\theta \\ &+ \int_{\theta_B}^{\theta_C}\int_{-R}^{R}\int_0^{\sqrt{R^2-y^2}} (r_m+y)^2\sin\theta dxdyd\theta \\ &+ \int_{\theta_C}^{\theta_D}\int_{-R}^{d_2}\int_0^{\sqrt{R^2-y^2}} (r_m+y)^2\sin\theta dxdyd\theta \Bigg]\end{aligned} \tag{25}$$

The iterative method is employed in this work to obtain the results, and the method's flow chart is illustrated in Figure 2. When the external work rate is greater than the internal dissipation work rate, i.e., $\dot{W}_\gamma > \dot{D}$, $\sigma_c > 0$, it means that the tunnel face is in an unstable condition, another face pressure needs to be applied, and at this time the FS_2 should be replaced by the average value. On the contrary, when the external work rate is less than the internal dissipation work rate, i.e., $\dot{W}_\gamma < \dot{D}$, $\sigma_c < 0$, it means that the tunnel face is in a stable condition, there is no need to apply additional support pressure, and at this time FS_1 should be replaced by the average value. When the value of σ_c is less than 0.01 kPa, or the difference between FS_1 and FS_2 is less than 0.001, the iteration ends.

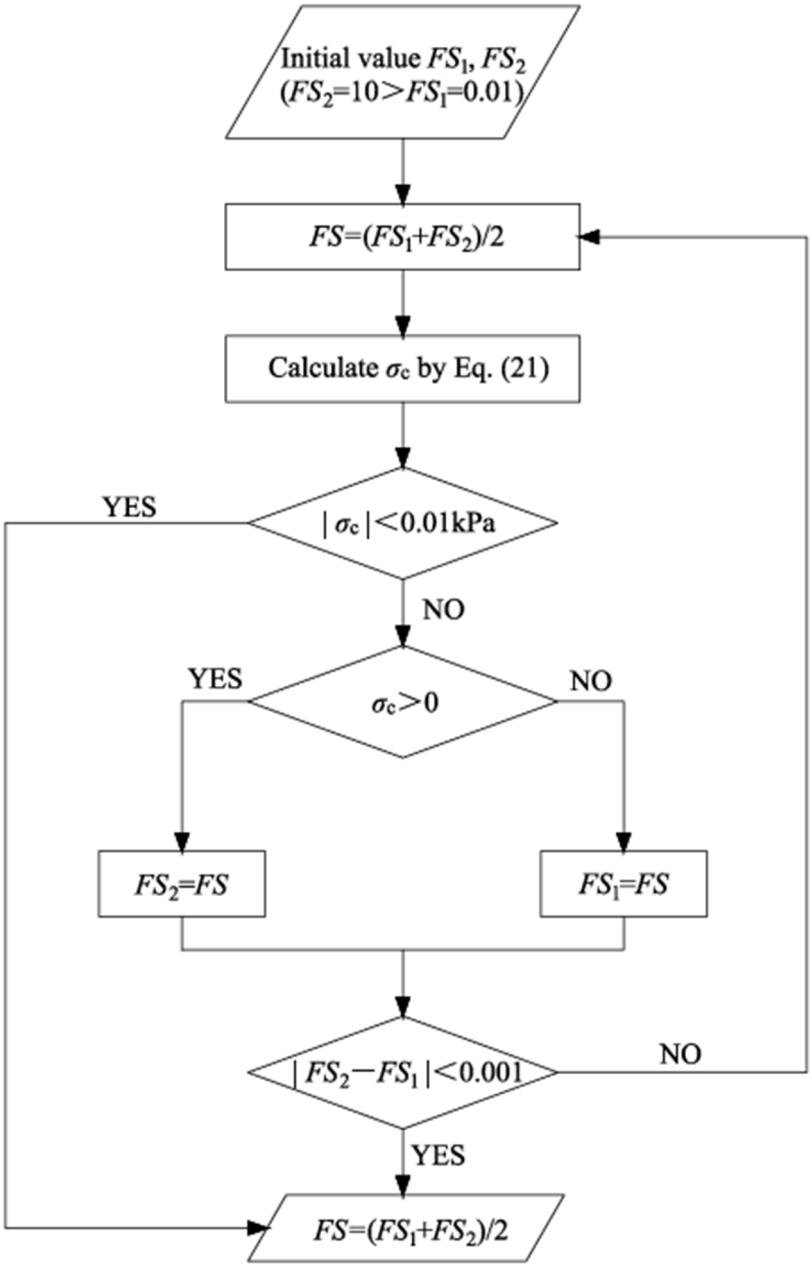

Figure 2. Iterative flow diagram for calculating the safety factor.

5. Results and Discussion

5.1. Parameter Selection

To analyze the face stability for a tunnel under conditions of steady unsaturated seepage and soil inhomogeneity, certain parameters need to be clarified. The parameters for the case of steady unsaturated seepage include the following: soil pore parameter n, soil entry pressure parameter $\alpha(\mathrm{kPa}^{-1})$, saturated hydraulic conductivity $k_s(\mathrm{m/s})$, flow rates $q(\mathrm{m/s})$. Different soil types haves varying parameters as follows: clay: $n = 2$, $\alpha = 0.005$, $k_s = 5 \times 10^{-8}$; silt: $n = 3$, $\alpha = 0.01$, $k_s = 5 \times 10^{-7}$; loess: $n = 4$, $\alpha = 0.025$, $k_s = 1 \times 10^{-6}$; and sand: $n = 5$, $\alpha = 0.1$, $k_s = 3 \times 10^{-5}$. The above values come from Vahedifard et al. (2015) [15]. The range of flow rates q varies from -3.14×10^{-8} to 1.15×10^{-8}, high evaporation corresponds to 1.15×10^{-8}, high infiltration corresponds to -3.14×10^{-8} and $q = 0$ corresponds to a no-flow condition (Li et al. 2019) [20]. The soil inhomogeneity parameter was chosen based on the premise that the effective cohesion of the soil at a depth of H, i.e., c′ in Equation (9),

was taken as the default value, in which the soil inhomogeneity was varied by changing n_0. In addition, the ratio of the tunnel depth to the tunnel excavation diameter is included as a geometric parameter in the discussion.

5.2. Parametric Studies

This paper analyzes the effect of several parameters on the face stability of the tunnel under steady unsaturated seepage and inhomogeneous soil conditions. The parameters can be found in Figure 1. Some of these parameters are set to fixed values as follows: $\varphi' = 20°$, at depth H = 10 m, $c' = 20$ kN/m^2 and $\gamma_w = 10$ kN/m^3.

5.2.1. Effects of Cover-to-Diameter Ratio (C/D)

Figure 3 shows that as the ratio of the tunnel depth to the diameter of the tunnel (C/D) increases, the safety factor FS increases, regardless of the type of soil. Further observation reveals that the slope of the curve increases as the C/D increases, i.e., the growth rate of the FS continues to increase. The reason for this phenomenon is that cohesion increases with depth when considering the inhomogeneity of the soil, and the increase in the C/D means that the depth of the tunnel relative to the diameter D increases, and the cohesion of the soil near the tunnel face also becomes larger, thus contributing to the growth rate of the FS. It is worth mentioning that the FS obtained with a further increase in the C/D will remain constant, because the failure mechanism only outcrops when the cover-to-diameter ratio (C/D) is small. The influence of the C/D varies with soil type as well; it can be found that the rate of increase of the FS is greater in clay than in silt, which in turn is greater than in loess and sand, which are basically the same. This phenomenon is not obvious in Figure 3a, but it is more pronounced in Figure 3b,c, i.e., under the conditions of no-flow and high evaporation.

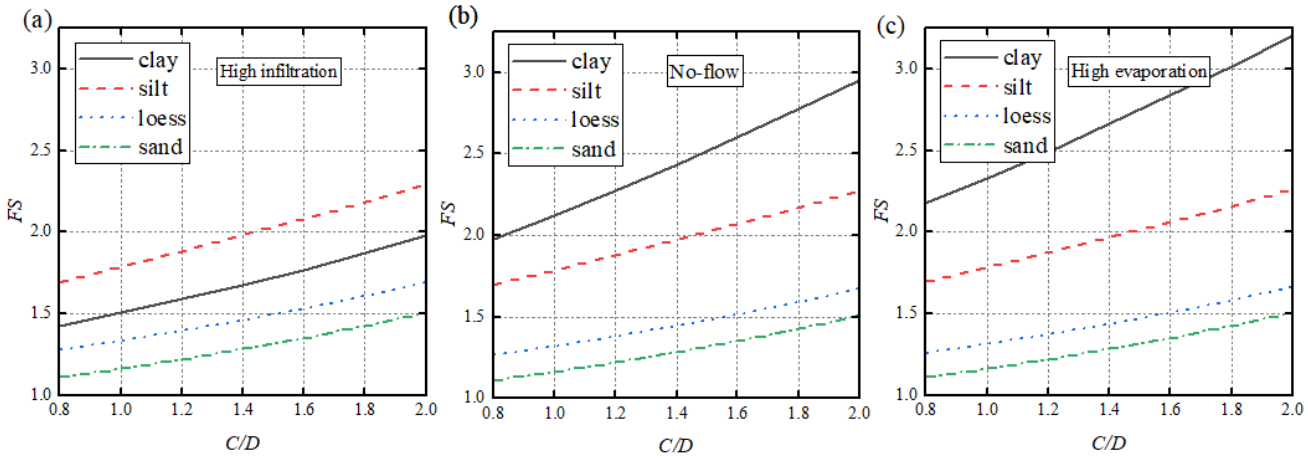

Figure 3. FS versus C/D for various soil types with $n_0 = 0.7$: (**a**) $q = -3.14 \times 10^{-8}$; (**b**) $q = 0$; (**c**) $q = 1.15 \times 10^{-8}$.

5.2.2. Effects of Flow Rates

As can be seen in Figure 4, the FS corresponding to silt, loess and sand remains essentially constant as the flow rate changes, and only the FS corresponding to clay increases sharply, which can be seen in Figures 3 and 5.

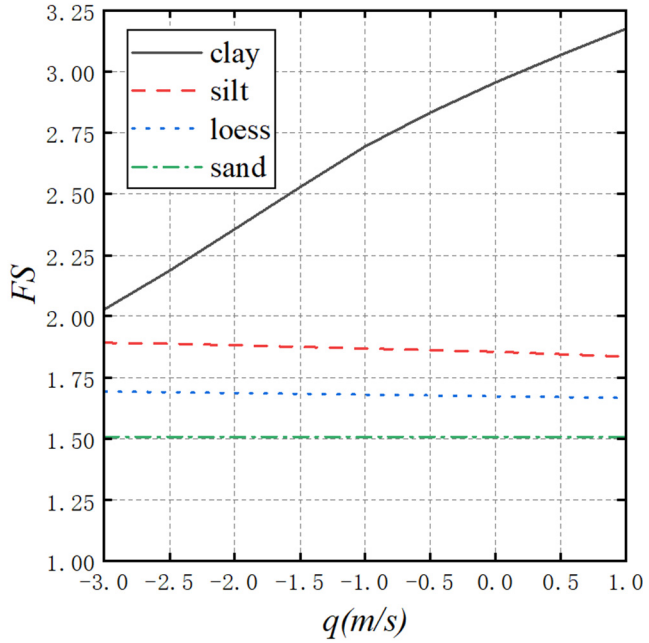

Figure 4. FS versus q for various soil type with C/D = 2, D = 10 m, n_0 = 0.7.

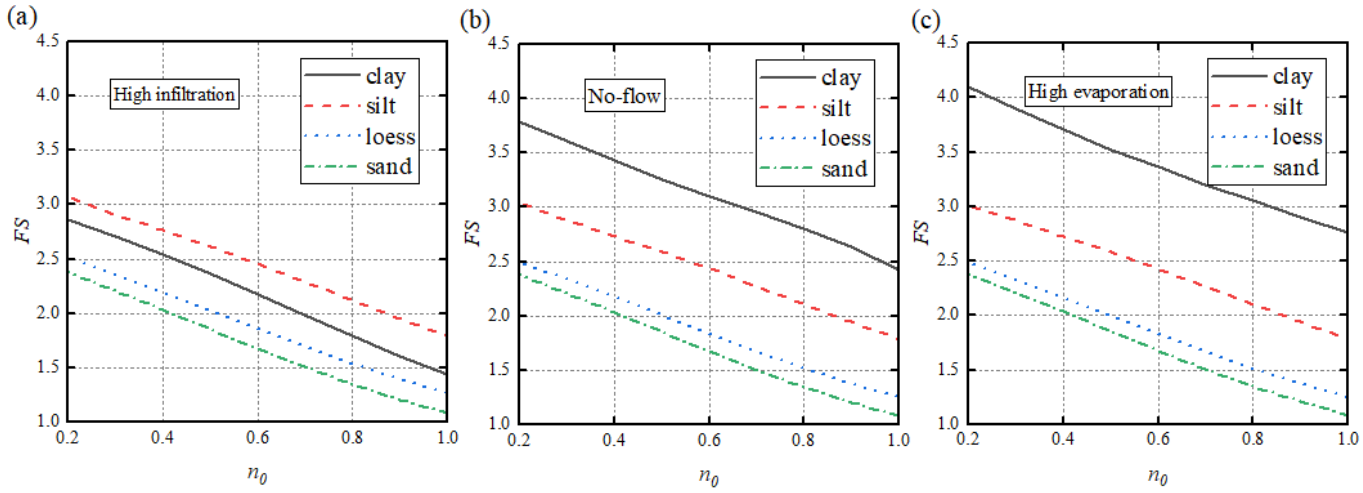

Figure 5. FS versus n_0 for different soil types with C/D = 2, D = 10 m: (**a**) high infiltration condition; (**b**) no-flow condition; (**c**) high evaporation condition.

5.2.3. Effects of Inhomogeneous Parameter

Figure 5 shows that as the inhomogeneity parameter n_0 increases, the safety factor decreases almost linearly. This occurs for the following reason: although the soil inhomogeneity leads to smaller soil cohesion near the ground surface, the cohesion increases linearly with depth, leading to larger soil cohesion near the tunnel face in deeper tunnels, and the log-spiral collapse model is a cone, most of which is located near the tunnel face; therefore, the larger cohesion near the face makes a positive contribution to the safety factor. In addition, for the same parameters, different safety factors are exhibited for different soil conditions; in most cases, clay has the highest safety factor, followed by silt, loess is third and sand is the lowest, but as can be seen in Figures 3 and 5, clay has a lower safety factor than silt only in the case of high infiltration.

6. Conclusions

In this paper, a model of steady unsaturated seepage is integrated with an inhomogeneous soil model, the internal work rate and external work rate are calculated based on a log-spiral collapse model, and kinematic methods and strength reduction techniques are used to obtain the safety factor, which is finally obtained by an iterative method in order to find zero support pressure. Eventually, a framework is established for analyzing the face stability of a tunnel under conditions of steady unsaturated seepage and soil inhomogeneity. Under the conditions explored in this paper, the main findings are as follows:

(1) Under steady unsaturated seepage conditions, the flow rate should be stable. However, this paper compares steady seepage at different flow rates and found that tunnel face stability in clay is sensitive to changes in flow rate; the remaining soil types, i.e., silt, loess, and sand, are virtually unaffected by flow rate changes.
(2) In most cases, tunnel faces in clay have the highest safety factor, followed by silt, while loess is third and sand has the lowest safety factor. It is worth mentioning that tunnel faces in clay have a lower safety factor than those in silt only in the case of high infiltration.
(3) The influence of the cover-to-diameter ratio C/D of the tunnel on the stability of the tunnel face in various soil types is as follows: clay $>$ silt $>$ loess $>$ sand.
(4) The soil's inhomogeneity significantly affects the stability of the tunnel face. Different types of soils have different unsaturated seepage conditions, and coupled with the variation of flow rate, these also affect the stability of the tunnel face. Consideration of steady unsaturated seepage and inhomogeneity conditions in the design can effectively improve the stability of the tunnel face.

This paper provides a methodology to analyze tunnel face stability in the conditions of steady unsaturated seepage and soils with conditions of inhomogeneity, however, the present work ignores many details, such as the effect of saturation, the inhomogeneous variations in layered soils, seismic effects, overconsolidation of soils, etc.; these conditions also deserve to be considered.

Author Contributions: Methodology, Y.X.; resources, D.Z. and H.L.; date curation, Y.X.; writing—original draft, Y.X.; writing—review and editing, D.Z. and H.L.; supervision, D.Z. and H.L. All authors have read and agreed to the published version of the manuscript.

Funding: This research received no external funding.

Institutional Review Board Statement: Not applicable.

Informed Consent Statement: Not applicable.

Data Availability Statement: The data analyzed are available from the corresponding author on reasonable request. The data are not publicly available due to reasons of privacy.

Conflicts of Interest: The authors declare no conflicts of interest.

References

1. Mollon, G.; Dias, D.; Soubra, A.H. Face stability analysis of circular tunnels driven by a pressurized shield. *J. Geotech. Geoenviron. Eng.* **2010**, *136*, 215–229. [CrossRef]
2. Subrin, D.; Wong, H. Tunnel face stability in frictional material: A new 3D failure mechanism. *Comptes Rendus Mec.* **2002**, *330*, 513–519. [CrossRef]
3. Mollon, G.; Dias, D.; Soubra, A.H. Rotational failure mechanisms for the face stability analysis of tunnels driven by a pressurized shield. *Int. J. Numer. Anal. Methods Geomech.* **2011**, *35*, 1363–1388. [CrossRef]
4. Oreste, P.P.; Dias, D. Stabilisation of the excavation face in shallow tunnels using fibreglass dowels. *Rock Mech. Rock Eng.* **2012**, *45*, 499–517. [CrossRef]
5. Perazzelli, P.; Leone, T.; Anagnostou, G. Tunnel face stability under seepage flow conditions. *Tunn. Undergr. Space Technol.* **2014**, *43*, 459–469. [CrossRef]
6. Yang, X.L.; Yin, J.H. Slope stability analysis with nonlinear failure criterion. *J. Eng. Mech.* **2004**, *130*, 267–273. [CrossRef]
7. Yang, X.L.; Huang, F. Collapse mechanism of shallow tunnel based on nonlinear Hoek–Brown failure criterion. *Tunn. Undergr. Space Technol.* **2011**, *26*, 686–691. [CrossRef]

8. Yang, X.L.; Yin, J.H. Upper bound solution for ultimate bearing capacity with a modified Hoek–Brown failure criterion. *Int. J. Rock Mech. Min. Sci.* **2005**, *42*, 550–560. [CrossRef]
9. Yang, X.L.; Wang, J.M. Ground movement prediction for tunnels using simplified procedure. *Tunn. Undergr. Space Technol.* **2011**, *26*, 462–471. [CrossRef]
10. Xu, S.; Liu, J.; Yang, X.L. Pseudo-dynamic analysis of a 3D tunnel face in inclined weak strata. *Undergr. Space* **2023**, *12*, 156–166. [CrossRef]
11. Yang, X.L.; Li, L.; Yin, J.H. Seismic and static stability analysis for rock slopes by a kinematical approach. *Geotechnique* **2004**, *54*, 543–549. [CrossRef]
12. Zhang, Z.L.; Wu, Y.M. A general kinematic approach to the seismic stability assessment of slopes. *Comput. Geotech.* **2023**, *160*, 105519. [CrossRef]
13. Li, L.C.; Tang, C.A.; Zhu, W.C.; Liang, Z.Z. Numerical analysis of slope stability based on the gravity increase method. *Comput. Geotech.* **2009**, *36*, 1246–1258. [CrossRef]
14. Lu, N.; Godt, J.W.; Wu, D.T. A closed-form equation for effective stress in unsaturated soil. *Water Resour. Res.* **2010**, *46*, W05515. [CrossRef]
15. Vahedifard, F.; Leshchinsky, B.A.; Mortezaei, K.; Lu, N. Active earth pressures for unsaturated retaining structures. *J. Geotech. Geoenviron. Eng.* **2015**, *141*, 04015048. [CrossRef]
16. Nian, T.K.; Chen, G.Q.; Luan, M.T.; Yang, Q.; Zheng, D.F. Limit analysis of the stability of slopes reinforced with piles against landslide in nonhomogeneous and anisotropic soils. *Can. Geotech. J.* **2008**, *45*, 1092–1103. [CrossRef]
17. Lu, N.; Likos, W.J. *Unsaturated Soil Mechanics*; Wiley: Hoboken, NJ, USA, 2004.
18. Griffiths, D.V.; Lu, N. Unsaturated slope stability analysis with steady infiltration or evaporation using elasto-plastic finite elements. *Int. J. Numer. Anal. Methods Geomech.* **2005**, *29*, 249–267. [CrossRef]
19. Pan, Q.; Dias, D. Face stability analysis for a shield-driven tunnel in anisotropic and nonhomogeneous soils by the kinematical approach. *Int. J. Geomech.* **2016**, *16*, 04015076. [CrossRef]
20. Li, Z.W.; Yang, X.L.; Li, T.Z. Face stability analysis of tunnels under steady unsaturated seepage conditions. *Tunn. Undergr. Space Technol.* **2019**, *93*, 103095. [CrossRef]